JOURNAL OF PROPULSION AND POWER
Vol. 17, No. 2, March–April 2001

Periodic Propellant Flames and Fluid-Mechanical Effects

T. L. Jackson,* J. Buckmaster,† and A. Hegab‡
University of Illinois at Urbana–Champaign, Urbana, Illinois 61801

We construct the combustion field generated by a periodic reactant supply that models the supply from a heterogeneous propellant. A full accounting of the fluid mechanics is incorporated. However, solutions differ little from those generated asssuming a uniform mass flux (the constant density model). On the other hand, allowing for temperature-dependent transport (power law or Sutherland's law) strongly affects the reaction rate and the heat flux to the propellant surface. The effects of nonuniform mass flux at the propellant surface are discussed, such nonuniformity arising, for example, because of the different densities of the oxidizer and binder. And we discuss the effects of hills and valleys in the propellant surface.

Nomenclature

D	=	Damköhler number
e	=	internal energy
h	=	enthalpy
L	=	half-period of the grain
M	=	mass flux
$\mathcal{M}$	=	Mach number
p	=	pressure
T	=	temperature
T_{BS}	=	Burke–Schumann flame temperature
u, v	=	velocity components
X	=	mass fraction of oxidizer (gas phase)
Y	=	mass fraction of fuel (gas phase)
β	=	supply stoichiometric ratio
δ	=	scaled Damköhler number
μ	=	viscosity
$()_0$	=	surface values

Introduction

THERE has long been an interest in understanding the nature of the combustion field supported by a heterogeneous propellant, and there have been many important contributions to this subject. Notable is the flame structure proposed by Beckstead, Derr, and Price (the BDP model[1]), and various improvements of this, e.g., Refs. 2 and 3, and a number of one-dimensional models, e.g., Refs. 4–6.

The BDP model is characterized by a deflagration sitting over the ammonium perchlorate (AP), a primary diffusion flame supported by AP and binder gases and the final diffusion flame supported by AP deflagration products and binder gases. A significant correction to this picture is implicit in the recognition by Price, Lee, and colleagues[7] of what he calls the leading-edge-flame and what one of us, in a general combustion context, calls the edge-flame.[8,9] This is the edge structure—a region where reactant mixing is important, neither a deflagration nor a diffusion flame—that exists when a diffusion flame has an edge. In the propellant context this edge occurs because the diffusion flame cannot extend all of the way to the surface, the temperature there being too low. The maximum reaction rate within the edge-flame is greater than in the trailing diffusion flame.

A second correction to the BDP picture is implicit in the results of elementary flame modeling.[10,11] The use of flux conditions at the propellant surface (rather than Dirichlet data) together with the stoichiometric requirement for large amounts of oxidizer causes the stoichiometric level surface (SLS) in a mixture-fraction formulation to intersect the surface on the AP, not at the AP/binder boundary, and the diffusion flames must lie on the SLS, if it is assumed that the oxidizer and fuel Lewis numbers are equal.

A third correction, long recognized, is apparent when one examines the nature of a typical AP mix. Miller[12] describes the propellant SD-1-88-17, for example, consisting of 30% by weight of 90 micron AP particles and 40% by weight of 20 micron particles. Of course, the distribution is not bimodal. In a typical 20 micron AP batch examined at the Thiokol Corporation (private communication with R. Bennett, March 2000), 30% by weight is smaller than 7 microns; overall there is a heavy bias in the distribution toward fine powder. This powder, mixed with the binder, will generate a fuel-rich mixture near the surface that can support a deflagration, rather than individual diffusion flames. (The disappearance of the SLS for small Peclet number particles is discussed in Ref. 11.)

What these various corrections or modifications suggest is that real propellant flames are complex creatures whose structure cannot reliably be guessed, even with substantial physical insights. There is no substitute for numerical simulations.

We have published a number of papers[11,13,14] (see also Ref. 15) that examine simple models relevant to the combustion field which is supported by a heterogeneous propellant, part of a systematic study of this subject, of ever-increasing complexity. Our goal is to describe the three-dimensional combustion field, accounting for AP deflagration and AP/binder reaction, the nonuniform regression of the propellant surface, nonuniform mass flux from the surface (particularly that arising from the fact that the AP density is roughly double that of the binder), the hills and valleys in the propellant surface arising from the nonuniform regression, heat conduction within the solid, the effects of pressure and velocity fluctuations in the chamber gases, etc. Among other things this requires the numerical description of the random propellant morphology (a packing model), something that has not yet been addressed by the community. (The work of Ref. 16 is an exception, but morphologies are not explicitly described.)

The general problem is a difficult one, and we are engaged in an incremental approach partly designed to explore the various physical ingredients, to gain some sense of what is important and what might not be. An example is the analysis of Ref. 13 in which the effects of a shear flow on an isolated AP/binder flame are examined, and it is shown that there is a significant effect on the heat flux to the surface. It could be argued that this is relevant to the heat flux near the boundaries of large AP particles randomly distributed in a three-dimensional propellant. On the other hand, similar calculations (not reported) carried out for a periodic propellant of the kind discussed in Ref. 14 (and one that we examine in the present paper) reveal a negligible effect. Which result is relevant to three-dimensional random propellants is not clear at this time. Should shear not be significant in the final analysis, it is unlikely, in our opinion, that

Received 24 July 1999; revision received 6 June 2000; accepted for publication 12 June 2000.

*Senior Research Scientist, Center for the Simulation of Advanced Rockets, 1304 West Springfield Avenue; tlj@csar.uiuc.edu.

†Professor, Department of Aeronautical and Astronautical Engineering, 104 South Wright Street; limey@uiuc.edu.

‡Postgraduate Associate, Department of Aeronautical and Astronautical Engineering, 104 South Wright Street; hegab@uiuc.edu.

erosive burning can be attributed to the penetration of turbulence to the wall vicinity with a concomitant enhancement of diffusivity (the mixing length phenomenon). The flame structure sits very close to the surface, and it is difficult to see how eddies, small on this scale, could penetrate undissipated against the convective flow from the surface. A more likely scenario is that large eddies drive the flame toward the surface in some regions, pull it back in others, and the net effect on the heat flux averaged over an area greater than that characteristic of a single eddy is positive. These eddies might be generated by fluctuations in the flux from the surface associated with small-scale casting irregularities, or by the roll up of acoustically generated wall shear layers.[17,18] The calculation of the effect of various flow-fields on heterogeneous propellant flames is incomplete.

All of the work that we have done so far adopts the constant-density model. (This is standard terminology in the combustion community but perhaps misleading in the present context—see the later remarks.) In this model a solenoidal velocity field is assigned that affects the thermal field and the reactant fields, but fails to account for the effect of thermal expansion on the flowfield. This model is a useful one, of proven efficacy, but cannot be used in a true simulation, our ultimate goal, and so here we describe the first results obtained when a complete coupling between the combustion processes and the flowfield is accounted for. Specifically, we examine a one-dimensional periodic propellant that supports a two-dimensional combustion field, a sequel to the constant density study of Ref. 14.

As we have already noted in our discussion of the BDP model, even in the absence of metal particles there are several kinds of gas-phase flames in the combustion field of a heterogeneous propellant. One of these is the AP decomposition flame, essentially a one-dimensional deflagration that sits close to the AP surface. Its importance lies in the fact that much of the AP surface receives little heat from the other two flames,[14] and so it strongly controls the surface regression.

A second flame is the diffusion flame that is supported by binder gases and the products of the AP decomposition flame. Significant heat can be generated in this flame, but little, if any, is conducted back to the propellant surface, as its elements stand off too far from the surface. More precisely, the Peclet number based on the standoff distance of any element is large so that the convective heat flux directed away from the surface is much greater than the conductive heat flux directed toward the surface.

A third type of flame is the edge flame defined by the edge of the diffusion flame. Unbounded edge flames (also known, unfortunately, as triple flames, a locution that should be abandoned) have a well-defined propagation speed (positive or negative, according to the value of the Damköhler number[19,20]), and so it is useful, perhaps, to think of the edge flame as the component of the diffusion-flame/edge-flame duo that maintains the position of this duo in the wind from the propellant surface, although there are dangers in this view. The importance of the edge flame is that it provides the heat to the part of the surface which is not heated by the AP decomposition flame and so provides heat to the fuel binder. It can only perform this necessary service if the Peclet number defined by its standoff distance has order of magnitude one or smaller.

Our concern in the earlier work and in the present paper is with the edge flame, with its structure, shape, and position, and the surface heat flux that it generates. For that reason we do not include the model ingredients necessary to support the AP decomposition flame. Explicit justification for this comes if we assume that the AP flame is so close to the surface that it can be simply be regarded as a surface ingredient. And then, because we shall only examine the gas phase, imposing simple boundary conditions at the propellant surface, specification of the surface temperature being one of them, the role of the AP flame is merely implicit. It generates heat, but the sole impact of this heat is to sustain the prescribed surface temperature.

Coupling of the gas-phase/solid-phase processes is a crucial ingredient in the calculation of the surface regression but is something that we defer to a later study. In its stead, we specify the mass flux (not necessarily uniform) at the surface, and we explore a number of issues. We are concerned with the error introduced by using the constant density model, as it is an attractive tool for examining the three-dimensional problem, with the role played by temperature-dependent transport, with the effects of varying surface mass flux arising from the different densities of AP and binder, and with the effects of surface irregularites (hills and valleys) on the combustion field.

Constant-Density Model

It is useful to summarize the formulation of the constant density model before addressing the complete problem, as this enables us to introduce most of the model ingredients together with various convenient scalings in the context of a modest set of equations.

The specific details of the constant-density model for our problem are as follows: the density is set equal to a constant (so that the equation of state, Charles's law, is jettisoned); and a uniform velocity field $u = 0$, $v =$ constant is adopted, which satisfies both the continuity equation and the momentum equation. Then the mass flux ρv is constant, and the model is merely a variation on that proposed by Burke and Schumann in 1928 (Ref. 21). (An alternative and essentially equivalent formulation is to permit density variations via the equation of state, but set the mass flux equal to a constant, satisfying continuity but jettisoning the momentum equation). Then, with the adoption of one-step Arrhenius kinetics, the equations for the temperature T and the oxidizer X and fuel Y concentrations are

$$M\frac{\partial}{\partial x}(C_pT, X, Y) = \rho D\nabla^2(C_pT, X, Y) + (Q, -\alpha_X, -\alpha_Y)BXYe^{-E/RT} \tag{1}$$

where we have assumed that both Lewis numbers are equal to one.

These equations are nondimensionalized using L, the half-period of the periodic grain configuration, and T_0, the surface temperature (the temperature at $y = 0$). At the same time we write $X = \alpha_X\check{X}$, $Y = \alpha_Y\check{Y}$, and then

$$\frac{\partial}{\partial\check{x}}(\check{T}, \check{X}, \check{Y}) = \frac{1}{Pe}\check{\nabla}^2(\check{T}, \check{X}, \check{Y}) + D(\check{Q}, -1, -1)\check{X}\check{Y}e^{-\theta/\check{T}} \tag{2}$$

where

$$Pe = ML/\rho D, \qquad \check{Q} = Q/C_pT_0$$

$$D = \alpha_X\alpha_YBL/M, \qquad \theta = E/RT_0$$

It is convenient to write

$$D = \delta e^{20} \tag{3}$$

In all calculations of the present type, the Peclet number Pe plays a vital role, and it is noteworthy that this role is not discussed in the most recent compilation of solid propellant combustion theory.[22]

The periodic propellant configuration is shown in Fig. 1. Boundary conditions are applied at the surface $\check{y} = 0$ and are

$$\check{T} = 1, \qquad \check{X} - \frac{1}{Pe}\frac{\partial\check{X}}{\partial\check{y}} = \check{X}_s \quad \text{or} \quad 0$$

$$\check{Y} - \frac{1}{Pe}\frac{\partial\check{Y}}{\partial\check{y}} = \check{Y}_s \quad \text{or} \quad 0 \tag{4}$$

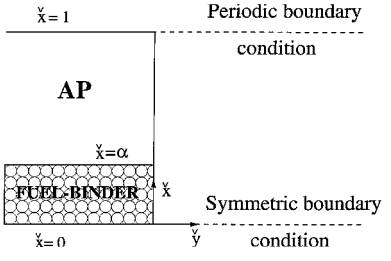

Fig. 1 Periodic propellant configuration.

where $\check{X}_s = X_s/\alpha_X$, $\check{Y}_s = Y_s/\alpha_Y$, and X_s is the fraction of AP that is X and Y_s is the fraction of binder that is Y. Equations (4b) and (4c) are flux conditions and the choices on the right-hand side are made according to whether the surface is AP ($\alpha < \check{x} < 1$) or binder ($0 \le \check{x} < \alpha$).

An important parameter is

$$\beta = \check{Y}_s/\check{X}_s = \alpha_X Y_s/\alpha_Y X_s \tag{5}$$

the ratio of the solid AP to solid binder required for stoichiometric combustion. To see this, an amount of solid AP equal to $\alpha_X Y_s$ generates $\alpha_X X_s Y_s$ of X, and an amount of binder equal to $\alpha_Y X_s$ generates $\alpha_Y X_s Y_s$ of Y. β is an assigned parameter, closer to 10 than to 1 for real propellants, and we have typically made the choice $\beta = 7$.

The actual supply ratio of AP to binder is $(1-\alpha)/\alpha$, and this is equal to β if the supply is stoichiometric, corresponding to a value of α:

$$\alpha_s = 1/(1+\beta) \tag{6}$$

Should α be larger than α_s, the supply will be fuel rich; should α be smaller than α_s, the supply will be fuel lean.

It is clear that an arbitrary choice can be made for α_Y because only the ratios $\check{Q}/\alpha_Y$ and α_X/α_Y control the solution. Thus $\check{Y}_s$ can be arbitrarily assigned, and for consistency with Ref. 14 we make the choice

$$\check{Y}_s = 0.4(1+\beta) \tag{7}$$

This arises in a natural way in Ref. 14 because of the way the equations are nondimensionalized there, different from what has been done here.

With $\check{Y}_s$ assigned, $\check{X}_s$ is determined by the choice of β, and $\check{Q}$ is chosen to generate a suitable flame temperature. The Burke–Schumann flame temperature defined by two quarter-planes of propellant[11] is

$$\check{T}_{\mathrm{BS}} = 1 + \check{Q}\check{X}_s\check{Y}_s/(\check{X}_s + \check{Y}_s) \tag{8}$$

and this can be used to select a suitable $\check{Q}$.

Figures 2 and 3 show typical solutions, obtained for parameter choices $\theta = 30$, $\check{Q} = 5$, $\beta = 7$, $\delta = 0.1$, $Pe = 5$, and $\alpha = \frac{1}{8}$. The flame

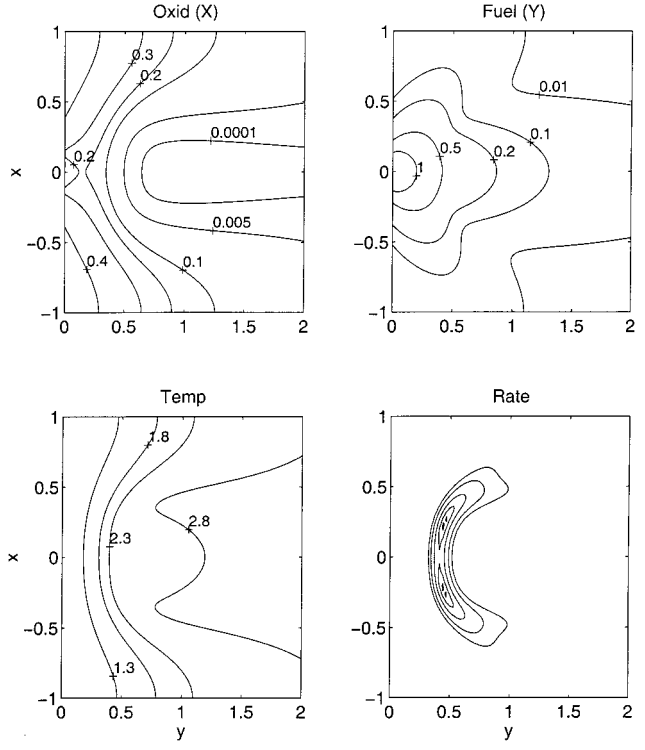

Fig. 2 Constant density solution: X, Y, T, RR contours; $\theta = 30$, $\check{Q} = 5$, $\beta = 7$, $\delta = 0.1$, $Pe = 5$, $\alpha = 1/8$; RR contours: 3.5, 3, 2, 1, 0.5.

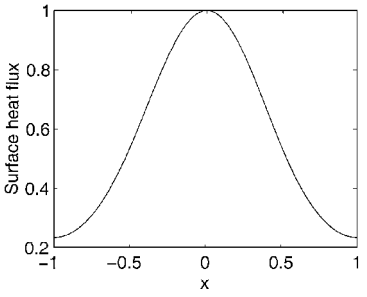

Fig. 3 Surface heat flux $-\partial\check{T}/\partial y(\check{x}, 0)$, constant density solution (see Fig. 2).

is characterized by two strong mixing structures each centered at $|\check{x}| \approx 0.2$ and surface heat flux concentrated at $\check{x} = 0$, the center of the fuel binder, with little at $\check{x} = 1$, the center of the AP. As we noted earlier, this makes clear the importance of the AP decomposition flame in determining the overall regression rate.

Variable Density Model

When full fluid-mechanics coupling is accounted for, the system of equations (2) is replaced by (with the checkmark dropped)

$$\frac{\partial \boldsymbol{F}}{\partial x} + \frac{\partial \boldsymbol{G}}{\partial y} = \frac{\partial \boldsymbol{F}_v}{\partial x} + \frac{\partial \boldsymbol{G}_v}{\partial y} + \boldsymbol{S} \tag{9}$$

where the convective flux vectors are given by

$$\begin{aligned}\boldsymbol{F} &= (\rho u,\ \rho u^2 + p/\gamma\mathcal{M}^2,\ \rho uv,\\ &\quad u\{\rho e + [(\gamma-1)/\gamma]p\},\ \rho uY,\ \rho uX)^T\\ \boldsymbol{G} &= (\rho v,\ \rho uv,\ \rho v^2 + p/\gamma\mathcal{M}^2,\\ &\quad v\{\rho e + [(\gamma-1)/\gamma]p\},\ \rho vY,\ \rho vX)^T\end{aligned} \tag{10}$$

the diffusive flux vectors by

$$\begin{aligned}\boldsymbol{F}_v &= \left[0,\ \tau_{xx},\ \tau_{xy},\ (\gamma-1)\mathcal{M}^2(u\tau_{xx} + v\tau_{xy})\right.\\ &\quad \left. + \frac{\mu Sc}{Pr\,Pe}\frac{\partial T}{\partial x},\ \frac{\mu}{Pe}\frac{\partial Y}{\partial x},\ \frac{\mu}{Pe}\frac{\partial X}{\partial x}\right]^T\\ \boldsymbol{G}_v &= \left[0,\ \tau_{xy},\ \tau_{yy},\ (\gamma-1)\mathcal{M}^2(u\tau_{xy} + v\tau_{yy})\right.\\ &\quad \left. + \frac{\mu Sc}{Pr\,Pe}\frac{\partial T}{\partial y},\ \frac{\mu}{Pe}\frac{\partial Y}{\partial y},\ \frac{\mu}{Pe}\frac{\partial X}{\partial y}\right]^T\end{aligned} \tag{11}$$

and the source term by

$$\boldsymbol{S} = [0, 0, 0, 0, Q, -1, -1]^T\Omega \tag{12}$$

The normal and shear stresses are

$$\begin{aligned}\tau_{xx} &= \frac{2\mu Sc}{Pe}\left[\frac{\partial u}{\partial x} - \frac{1}{3}\left(\frac{\partial u}{\partial x} + \frac{\partial v}{\partial y}\right)\right]\\ \tau_{yy} &= \frac{2\mu Sc}{Pe}\left[\frac{\partial v}{\partial y} - \frac{1}{3}\left(\frac{\partial u}{\partial x} + \frac{\partial v}{\partial y}\right)\right]\\ \tau_{xy} &= \frac{\mu Sc}{Pe}\left[\frac{\partial u}{\partial y} + \frac{\partial v}{\partial x}\right]\end{aligned} \tag{13}$$

and the internal energy equation and the equation of state are

$$e = T/\gamma + [(\gamma-1)/2]\mathcal{M}^2(u^2 + v^2), \qquad P = \rho T \tag{14}$$

Finally, the reaction rate is

$$\Omega = DXYe^{-\theta/T}, \qquad D = \delta e^{20} \tag{15}$$

In addition to the scales used for the constant-density model, we use the normal velocity at the surface V_0, the surface density ρ_0, the pressure $p_0 = \rho_0 R T_0$, and the viscosity μ_0. Now the Peclet number is $Pe = ML/\rho_0 D_0$ (constant), and other nondimensional parameters are the Schmidt number $Sc = \mu/\rho D$ (constant), the Prandtl number $Pr = \mu C_p/k$ (constant), and the Mach number $\mathcal{M} = V_0/c_0$. M is the dimensional mass flux $\rho_0 V_0$, and c_0 is the speed of sound $\sqrt{(\gamma p_0/\rho_0)}$.

In what follows we assume that the viscosity can have one of three forms:

Constant:

$$\mu = 1$$

Power law:

$$\mu = T^{0.7}$$

Sutherland's law:

$$\mu = aT^{\frac{3}{2}}/(b+T), \qquad a = 1+b \tag{16}$$

We shall compare results for all three cases, and for each case we shall take the Prandtl number to be either 1 or 0.7. The Schmidt number is always 1. The boundary conditions at the surface are as before, together with

$$u = 0, \qquad v = 1 \quad \text{at} \quad y = 0 \tag{17}$$

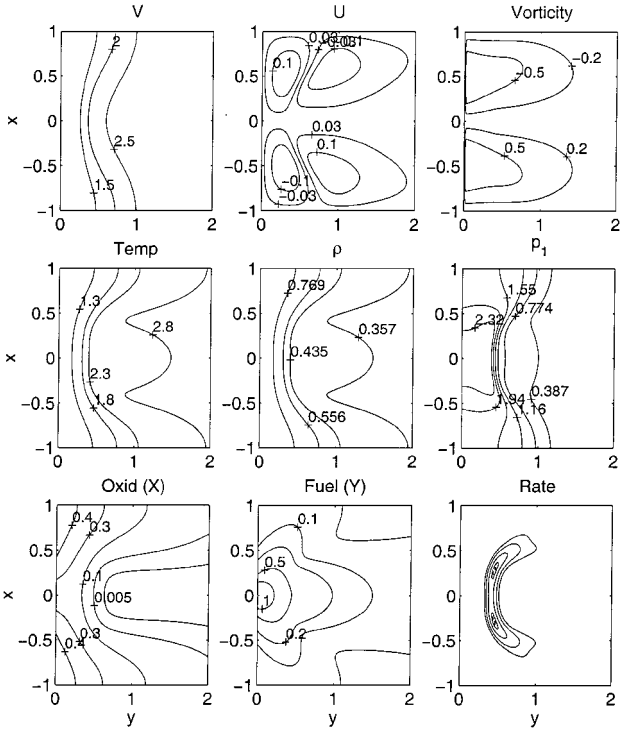

Fig. 4 Solution contours, variable density, $\mu = 1$, $\mathcal{M} = 0.01$, $\gamma = 1.2$, $Pr = Sc = 1$, other parameters as in Fig. 2. RR contours: 3.3, 3, 2, 1, 0.5.

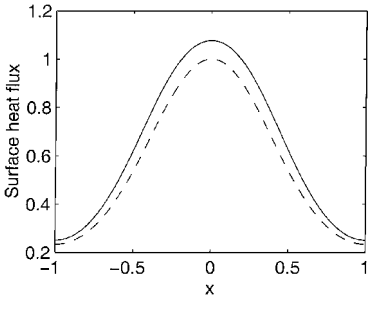

Fig. 5 Surface heat flux for Fig. 4 solution. The broken line is the constant density solution and is reproduced in later figures for comparative purposes.

in the case of uniform mass injection, or

$$\begin{aligned} u &= 0, \qquad v = 1 \quad \text{at} \quad y = 0, \qquad \alpha < |x| < 1 \\ u &= 0, \qquad v = 1/R_M \quad \text{at} \quad y = 0, \qquad |x| < \alpha \end{aligned} \tag{18}$$

when the injection velocity at the binder surface is different from the injection velocity at the AP surface. The rationalization for the latter choice originates in the fact that the specific gravity of AP is 1.95, that of a typical fuel binder 1.01 (Ref. 23) so that if we assume a flat regressing surface the mass flux through the AP surface is nearly double that through the fuel surface, and R_M should be assigned the value 1.95/1.01. In practice, of course, the surface will only be flat on average, and in due course we will need to account for surface irregularities, but a nonuniform surface mass flux is clearly a component of a complete simulation. With the choice (18), the stoichiometric value of α is

$$\alpha_s = 1/(1+\beta/R_M) \tag{19}$$

For the far-field condition as $y \to \infty$ we assume that u vanishes, the pressure $p = 1$, and the y derivatives of all other quantities vanish.

Numerical Method

Because we are interested in low Mach-number flows, we follow the numerical strategy outlined in Tseng and Yang.[24] To be more precise, we first define a reduced pressure

$$p = 1 + \gamma \mathcal{M}^2 p_1(x, y, t) \tag{20}$$

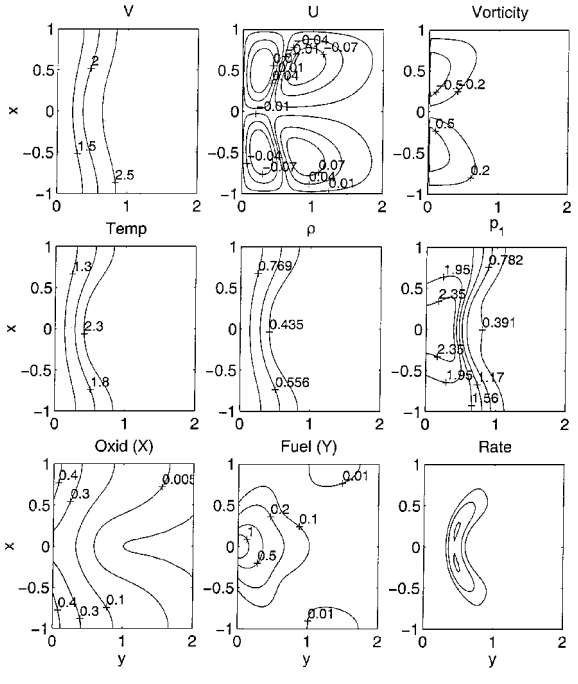

Fig. 6 Solution contours: variable density, power-law viscosity, other parameters as in Fig. 4. RR contours: 2, 1, 0.5.

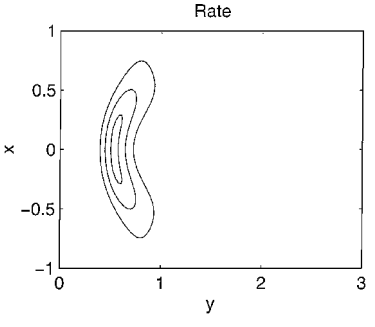

Fig. 7 RR contours: variable density, power-law viscosity, $Pr = 0.7$, other parameters as in Fig. 4; RR contours: 1.5, 1, 0.5.

and substitute into the equations of motion just given. The equation of state now becomes

$$\rho = \left(1 + \gamma \mathcal{M}^2 p_1\right)/T \tag{21}$$

and is used to update the density. Next, we add a pseudo-time derivative term of the form

$$\Gamma \frac{\partial \boldsymbol{Q}}{\partial \tau} \quad \text{where} \quad \boldsymbol{Q} = [p_1, u, v, h, Y, X]^T \tag{22}$$

to the governing equations, where τ is the pseudo-time, Γ is a preconditioner matrix added to accelerate convergence, and $h = T + \frac{1}{2}(\gamma - 1)\mathcal{M}^2(u^2 + v^2)$ is the enthalpy. We then march the solution to steady state (transient behavior has no meaning in pseudo-time). The code is stopped when the relative difference between solutions at two different time values is less than some prescribed tolerance, taken here to be 10^{-6}.

All numerical calculations were performed on a 160×100 grid, uniform in the x direction and stretched in the y direction. Convergence tests were carried out, and any further refinement resulted in less than 1% relative error.

Results

The first results we show are a test of the constant density model, and so we have taken $\mu = 1$, rather than one of the more realistic choices. The general expectation is that the constant density model does not lead to qualitative anomalies, but quantitative accuracy is not expected. For the present problem, however, a comparison of Fig. 4 with Fig. 2 reveals substantial qualitative agreement for T, X, Y and the reaction rate (RR). This is because u, the transverse velocity, is everywhere small so that the continuity equation forces a nearly uniform mass flux in the y direction. Absent some introduction of significant u variations by an applied shear,[13] significant deviations of the surface normal from the y direction, etc., the constant density model is accurate. Heat-flux predictions, for example, are in error by less than 10% (Fig. 5). In addition, the maximum temperature for variable ρ is 2.86 compared to 2.88 for the constant density solution, and the maximum RR ($RR_{\max}$) is 3.36 compared to 3.60 for the constant density solution. Thus the qualitative conclusions reached in Ref. 14 cannot be doubted merely because the constant density model was used.

An important corollary of these results is that we can, with reasonable confidence, explore certain aspects of the three-dimensional problem using the constant density model without fear of being led astray on this account.

The adoption of a more realistic viscosity law affects the solution of course, as there are then strong variations in all of the transport coefficients (μ, k, ρD) between the propellant surface and the main body of the flame. Figure 6 shows results that can be compared to Fig. 4 except that a viscosity power law is adopted. The differences appear modest for most variables, but now the maximum reaction rate is 2.12 (cf., 3.36 for Fig. 4). The differences in the maximum temperature are less sharp, 2.77 for Fig. 6 compared to 2.86 for Fig. 4. The $RR_{\max}$ ratio is 2.12/3.36 = 0.63, and the

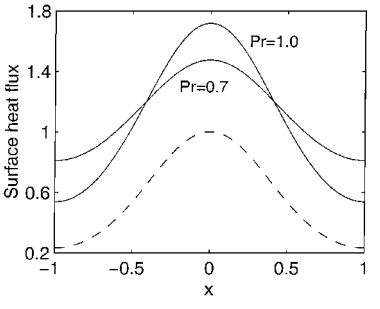

Fig. 8 Surface heat flux: variable density, power-law viscosity, *Pr* = 0.7, 1.0; other parameters as in Fig. 4.

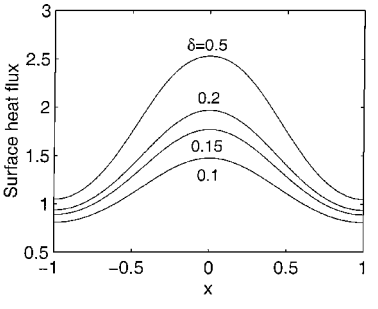

Fig. 10 Surface heat flux: variable density, power-law viscosity, various δ, *Pr* = 0.7, other data as in Fig. 4.

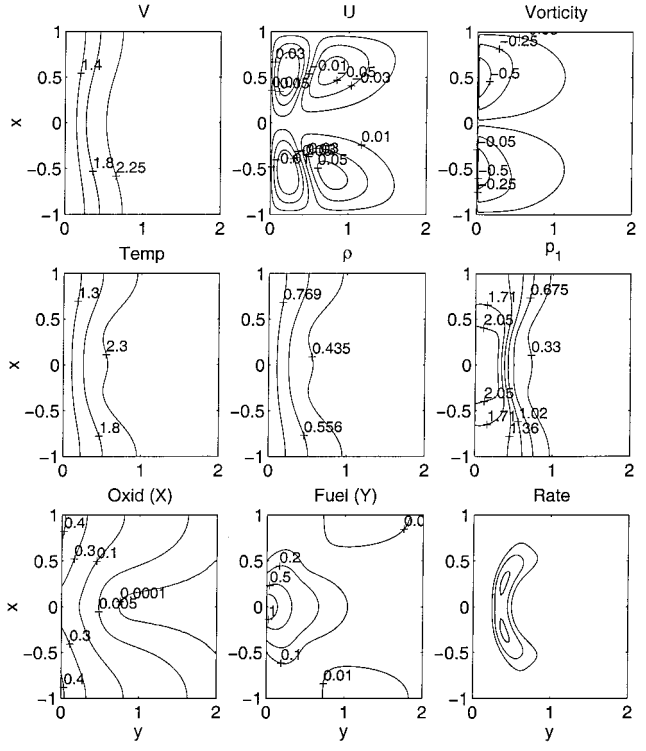

Fig. 9 Solution contours: variable density, $\delta = 0.5$, power-law viscosity, *Pr* = 0.7, other data as in Fig. 4.

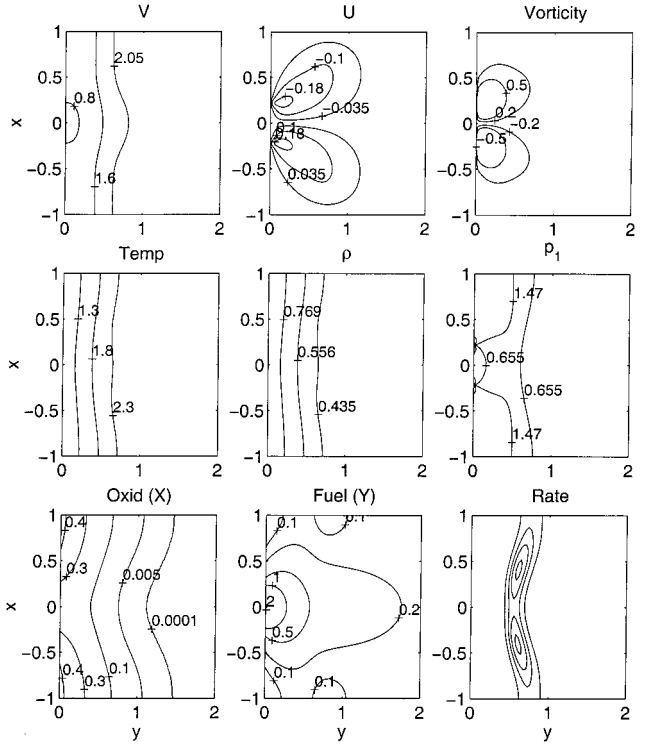

Fig. 11 Solution contours: uniform mass flux, power-law transport; RR contours: 2, 1, 0.5, cf. Fig. 6.

Arrhenius factor ratio is $\exp[-30/2.77+30/2.86]=0.7$, suggesting that the differences in maximum reaction rate arise because of differences in temperature.

Adjusting the Prandtl number has little affect on most of the contours, or on the maximum temperature, but a reduction of Pr to 0.7, all other parameters fixed at Fig. 6 values, reduces $RR_{\max}$ to 1.62 (Fig. 7).

Despite the significant reduction in $RR_{\max}$ in these calculations compared to that for $\mu=1$, and therefore a reduction in the maximum heat generation, the heat flux to the surface is increased by 50% or more (Fig. 8). An effect of decreasing Pr is to flatten out the distribution of this flux. These results make it clear that careful attention to modeling diffusive tranport will be important in detailed simulations and is more important for the present geometry than an accounting of two-way fluid coupling.

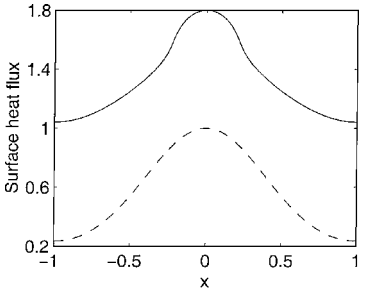

Fig. 12 Surface heat flux: A, full fluids model; B, constant density but temperature-dependent transport.

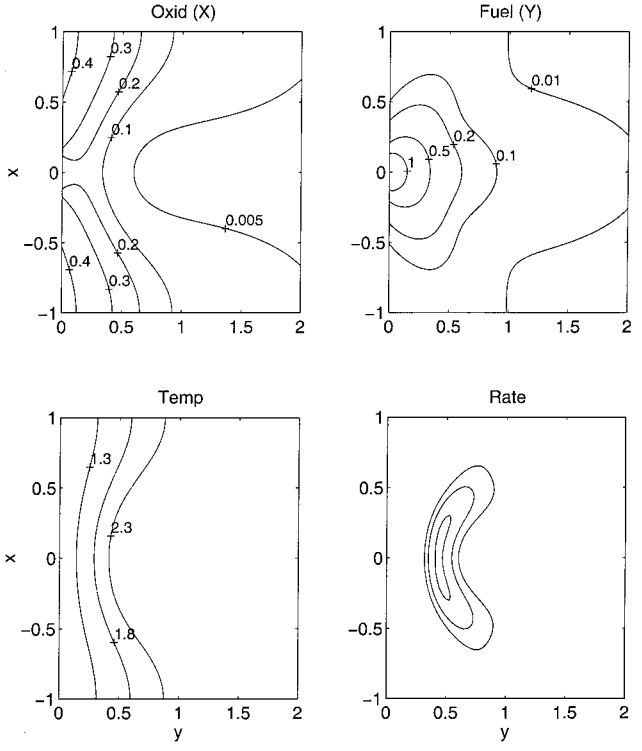

Fig. 13 Solution contours: nonuniform injection, $\alpha=\alpha_s$ [Eq. (19)], $\mu=1$, other parameters as in Fig. 4, RR contours: 3, 2, 1, 0.5.

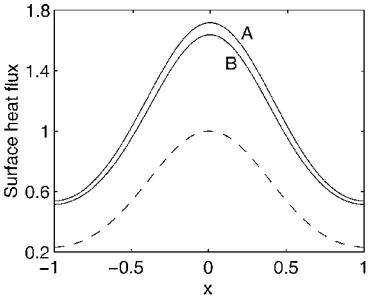

Fig. 14 Surface heat flux for the solution of Fig. 13.

An increase in the Damköhler number δ to 0.5 increases the vigor of the reaction and pushes the flame closer to the surface (Fig. 9). Now $RR_{\max}$ is 2.27, and $T_{\max}$ is 2.49. There is a correspondingly strong increase in the heat flux, as shown in Fig. 10, which also shows curves for $\delta=0.2$, 0.15, and 0.1.

Evidence that all of these solutions properly capture the low Mach-number flowfield, that the computational strategy permits calculations for arbitrarily small $\mathcal{M}$, comes from comparing results for $\mathcal{M}=0.01$ (Fig. 9) with those for $\mathcal{M}=0.001$, all other parameters fixed: $\mathcal{M}=0.01$: $RR_{\max}=2.26896$, $T_{\max}=2.48630$, $p_{1\max}=2.39787$; and $\mathcal{M}=0.001$: $RR_{\max}=2.26841$, $T_{\max}=2.48626$, $p_{1\max}=2.40483$. (Recall that $p=1+\gamma\mathcal{M}^2 p_1$ defines p_1.)

Calculations using Sutherland's law do not differ significantly from those using the power law, and we merely note the following values of $RR_{\max}$ and $T_{\max}$: 2.29 and 2.79 when $Pr=1$; 1.73 and 2.69 when $Pr=0.7$. (All other parameters as in Fig. 4.)

Constant Density, Temperature-Dependent Transport

Our results suggest that for the periodic propellant the use of the constant-density model does not introduce serious errors. The comparisons we have made, however, are for constant transport coefficients (Fig. 5). It is of interest, then, to see if the same conclusion can be drawn for the more physically relevant case of temperature-dependent transport. Figure 11 shows contours calculated when the mass flux is taken to be uniform, but a power law is adopted for the transport coefficients, results which are to be

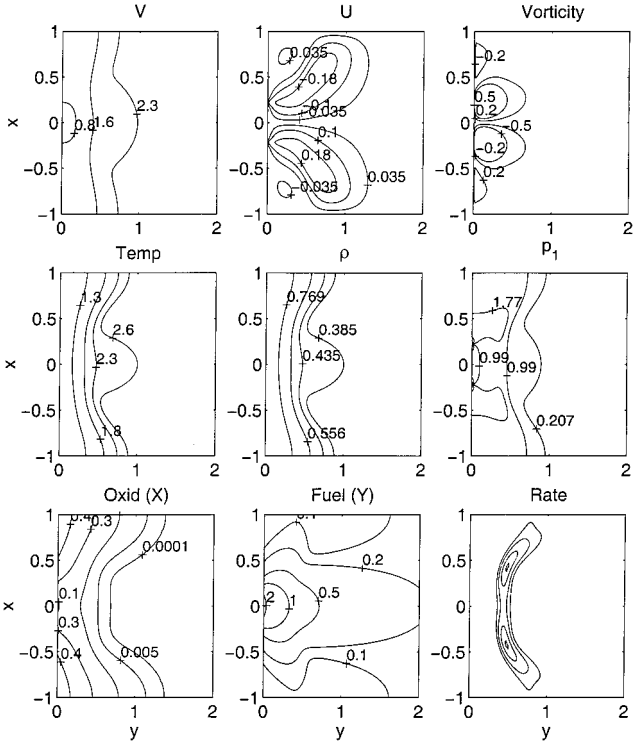

Fig. 15 Solution contours: nonuniform injection, power-law viscosity, $\alpha=\alpha_s$, $Pr=0.7$; RR contours: 1.2, 1, 0.8, 0.5.

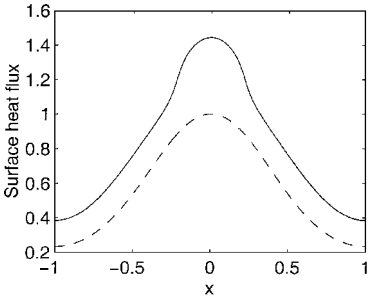

Fig. 16 Surface heat flux for Fig. 15.

compared directly to Fig. 6. The corresponding results for the heat flux are compared in Fig. 12. For the uniform mass flux RR_{max} is 2.2491, and the maximum temperature is 2.7951; for the full equations the corresponding results are 2.1175 and 2.7727. The differences are small.

Nonuniform Injection

We have carried out calculations similar to those just described but with the choice [Eq. (18)] for which the normal velocity at the fuel surface is ≈ 0.52 (but remains equal to 1 at the AP surface). Results for $\mu = 1$ (Fig. 13) show that the slow flow accelerates and v becomes more or less uniform in the neighborhood of the flame, with a positive bulge at the centerline downstream of the flame. The flame itself is substantially broadened compared to the uniform injection case (Fig. 4), but the surface heat flux is sharply enhanced to the fuel binder only (Fig. 14) because of the locally reduced Peclet number. RR_{max} is 3.13, compared to 3.60 for uniform injection, and T_{max} is 2.82 compared to 2.88 for uniform injection.

A power-law viscosity weakens the flame and increases the heat flux (Figs. 15 and 16). Moreover, the flame more closely resembles a plane deflagration here than it does for any of the other computations. (A plane deflagration is characteristic of small Peclet number calculations[14]). RR_{max} is 1.25 and T_{max} is 2.53.

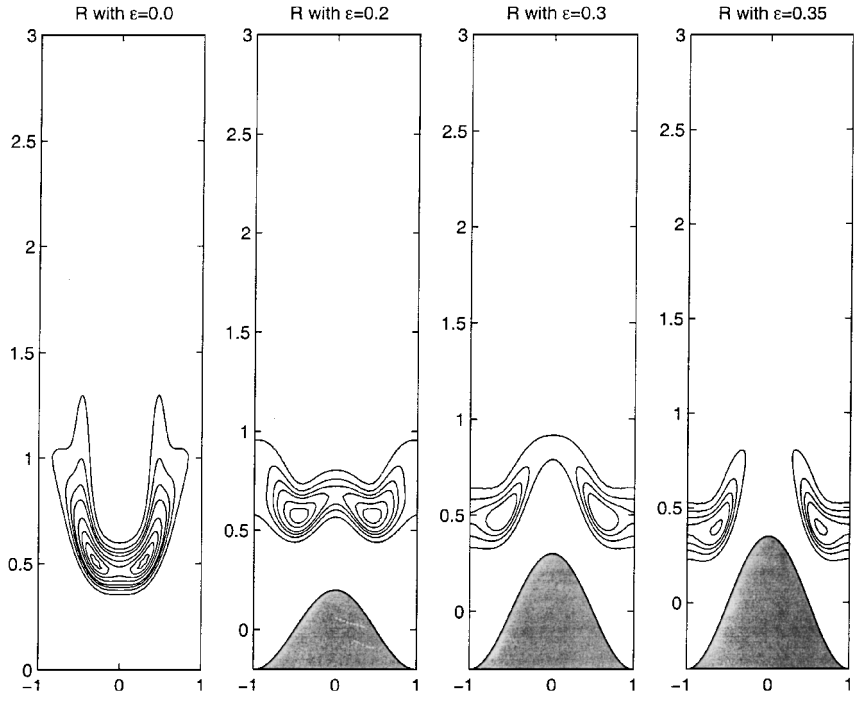

Fig. 17 RR contours, hills and valleys, case 1.

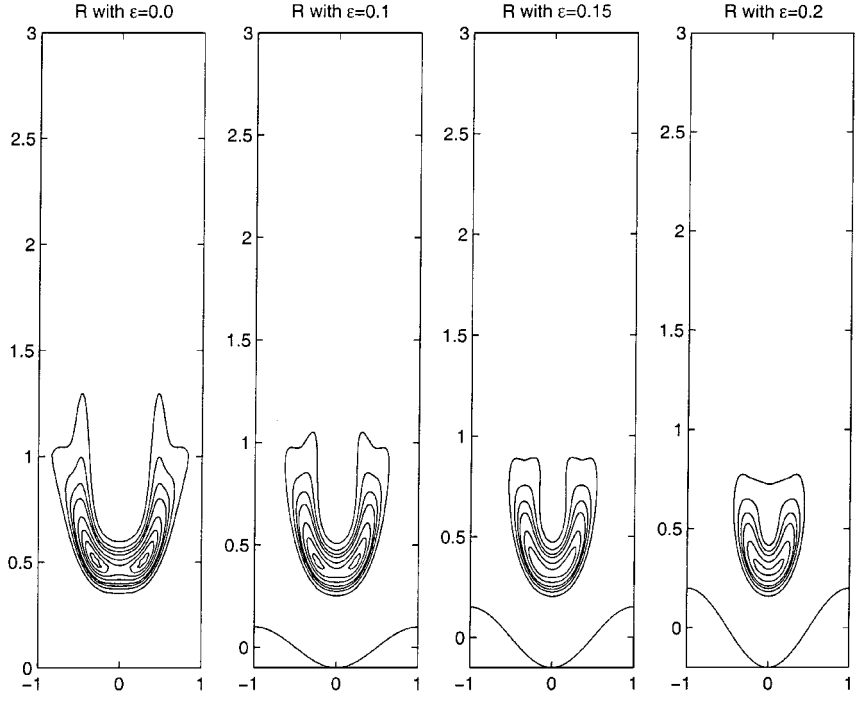

Fig. 18 RR contours, hills and valleys, case 1.

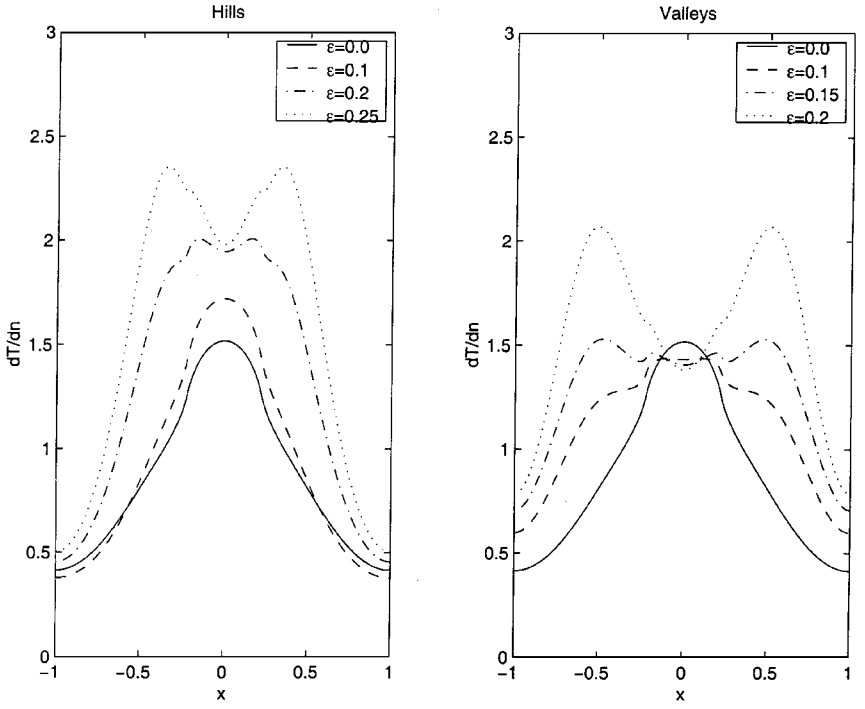

Fig. 19 Surface heat flux, hills and valleys, case 2.

Hills and Valleys

The final ingredient that we examine is that of a nonflat surface. Specifically, we suppose that the surface is located at

$$y = \pm\epsilon \cos(\pi x) \tag{23}$$

the plus sign corresponding to a hill centered on the binder at $x = 0$, and the minus sign to a hill centered on the AP at $|x| = 1$. Calculations have been done for the parameters used in Fig. 2 for two choices of mass flux at the surface: 1) M_n, the normal mass flux, equal to 1; 2) $M_n = \cos(\alpha)$ on the AP, $M_n = 1/R_M \cos(\alpha)$ on the binder, where α is the surface slope, $\tan(\alpha) = \mp\pi \sin(\pi x)$. In both cases the tangential velocity is zero. For case 1, mass conservation at the surface implies that the shape is changing. Case 2, on the other hand, corresponds to a constant regression of the surface at constant speed with unchanging shape. This is the probable late-time scenario for the periodic propellant, albeit with a shape that is determined by the gas/solid coupling and the surface physics, not assigned.

Figures 17 and 18 show results for case 1, for different values of ϵ. The vertical scale is greater than the horizontal scale. Figure 17 reveals not only significant effects on the shape of the flame, but also on the maximum reaction rate. When $\epsilon = 0$ all eight contour values are realized so that $RR_{\max} > 3$; but when $\epsilon = 0.3$, only four are realized so that $1.5 > RR_{\max} > 1$. Significant effects are also seen in Fig. 18. The general trend is similar for case 2, and we show the impact on the surface heat flux in Fig. 19. Our focus in the variety of calculations reported here has been on the surface heat flux because this drives the regression. Figure 19 suggests strongly that a complete simulation of heterogeneous propellant burning will not be accurate if surface unevenness is ignored.

Conclusions

There has been a great deal of interest in the past three decades and more in the details of heterogenous propellant combustion, but most modeling efforts have been one dimensional in nature, and those that are not have not been examined using numerical tools. Here, for the first time, we present two-dimensional calculations for a model that incorporates key ingredients of the combustion field with a full accounting of the fluid mechanics.

This is a sequel to earlier work[14] in which the Navier–Stokes equations were not used, and a constant mass flux was assigned. Important qualitative conclusions were drawn in the earlier work, and what we have shown here is that allowing for the influence of the thermal expansion on the flowfield has little effect on the solution when the surface is flat and the surface flux is uniform. We are presently engaged in calculating the three-dimensional combustion field supported by a propellant with two-dimensional surface variations, and the present results suggest that we will not have to include the fluid-mechanics coupling to draw useful qualitative conclusions. In this case the reduction in required computing resources is substantial.

Far more important than an accounting for the fluid-mechanics coupling is an accounting of temperature-dependent transport. If a power law or Sutherland's law is adopted for the viscosity-temperature dependence, with corresponding variations of the other transport coefficients, there is a significant increase in the heat flux to the propellant surface, a reduction in the maximum temperature, and a decrease in the maximum reaction rate.

It is tempting to consider modeling the propellant burning by assuming a flat surface and a uniform mass flux from that surface, as this is a substantial simplification. However, our results suggest that this could lead to serious quantitative error. Variations in mass flux associated with the density differences in the constituents (which therefore do not have a zero average) can strongly affect the combustion field. Surface unevenness likewise can have a large impact. Models which do not account for these phenomena might be useful, but results obtained from them should be interpreted with care.

Acknowledgments

The work of J. Buckmaster and A. Hegab is supported by U.S. Air Force Office of Scientific Research and by the U.S. Department of Energy through the University of California under subcontract number B341494. T. L. Jackson is supported by the latter agency.

References

[1]Beckstead, M. W., Derr, R. L., and Price, C. F., "A Model of Composite Solid-Propellant Combustion Based on Multiple Flames," *AIAA Journal*, Vol. 8, No. 12, 1970, pp. 2200–2207.

[2]Cohen, N. S., and Strand, L. D., "An Improved Model for the Combustion of AP Composite Propellants," *AIAA Journal*, Vol. 20, No. 12, 1982, pp. 1739–1746.

[3]Glick, R. L., "Distribution Functions for Statistical Analysis of Monodisperse Composite Solid Propellant Combustion," *AIAA Journal*, Vol. 14, No. 11, 1976, pp. 1631–1633.

[4]Cohen, N. S., "Review of Composite Propellant Burn Rate Modeling," *AIAA Journal*, Vol. 18, No. 3, 1980, pp. 277–293.

[5]Kerstein, A. R., "Percolation Model of Polydisperse Composite Solid Propellant Combustion," *Combustion and Flame*, Vol. 69, No. 1, 1987, pp. 95–112.

[6]Murphy, J., and Krier, H., "Linear Pressure Coupled Frequency Response of Heterogeneous Solid Propellants," *Proceedings of the Combustion Institute*, Vol. 27, No. 2, 1998, pp. 2343–2350.

[7]Lee, S. T., Price, E., and Sigman, R. J., "Effect of Multidimensional Flamelets in Composite Propellant Combustion," *Journal of Propulsion and Power*, Vol. 10, No. 6, 1994, pp. 761–768.

[8]Buckmaster, J., "Edge-Flames," *Journal of Engineering Mathematics*, Vol. 31, No. 2, 1997, pp. 269–284.

[9]Buckmaster, J., and Zhang, Yi., "Oscillating Edge-Flames," *Combustion Theory and Modelling*, Vol. 3, No. 3, 1999, pp. 547–565.

[10]Jia, X., and Bilger, R. W., "The Burke–Schumann Diffusion Flame with Zero Net Flux Boundary Conditions," *Combustion Science and Technology*, Vol. 99, No. 2, 1994, pp. 371–376.

[11]Buckmaster, J., Jackson, T. L., and Yao, J., "An Elementary Discussion of Propellant Flame Geometry," *Combustion and Flame*, Vol. 117, No. 3, 1999, pp. 541–552.

[12]Miller, R. R., "Effects of Particle Size on Reduced Smoke Propellant Ballistics," AIAA Paper 82-1096, June 1982.

[13]Buckmaster, J., and Jackson, T. L.,"The Effects of a Time-Periodic Shear on a Diffusion Flame Anchored to a Propellant," *Combustion and Flame*, Vol. 120, Nos. 1/2, 2000, pp. 211–221.

[14]Jackson, T. L., and Buckmaster, J., "Nonpremixed Periodic Flames Supported by Heterogeneous Propellants," *Journal of Propulsion and Power*, Vol. 16, No. 3, 2000, pp. 498–504.

[15]Buckmaster, J., and Jackson, T. L., "Response of Propellant Flames to Unsteady Flows, and Related Questions," AIAA Paper 99-0323, Jan. 1999.

[16]Davis, I. L., and Carter, R. G., "Random Particle Packing by Reduced Dimension Algorithms," *Journal of Applied Physics*, Vol. 67, No. 2, 1990, pp. 1022–1029.

[17]Roh, T-S., Apte, S., and Yang, V., "Transient Combustion Response of Homogeneous Solid Propellant to Acoustic Oscillations in a Rocket Motor," *Proceedings of the Combustion Institute*, Vol. 27, 1998, pp. 2335–2341.

[18]Lee, Y., and Beddini, R., "Acoustically Induced Turbulent Transition in Solid Propellant Rocket Chamber Flowfields," AIAA Paper 99-2058, June 1999.

[19]Dold, J. W., Hartley, L. J., and Green, D., "Dynamics of Laminar Triple-Flamelet Structures in Non-Premixed Turbulent Combustion," *Dynamical Issues in Combustion Theory*, edited by Paul C. Fife, A. Liñán, and F. Williams. Springer-Verlag, New York, 1991, pp. 83–105.

[20]Kioni, P. N., Rogg, B., Bray, K. N. C., and Liñán, A., "Flame-Spread in Laminar Mixing Layers: the Triple Flame," *Combustion and Flame*, Vol. 95, No. 2, 1993, pp. 276–290.

[21]Burke, S. P., and Schumann, T. E. W., "Diffusion Flames," *Industrial and Engineering Chemistry*, Vol. 20, No. 8, 1928, pp. 998–1004.

[22]*Nonsteady Burning and Combustion Stability of Solid Propellants*, edited by Luigi De Luca, Edward W. Price, and Martin Summerfield, Progress in Astronautics and Aeronautics, Vol. 143, AIAA, Washington, DC, 1992.

[23]*Rocket Propulsion Elements*, 6th ed., edited by George P. Sutton, Wiley, New York, 1992, p. 450.

[24]Tseng, I. S., and Yang, V., "Combustion of a Double-Base Homogeneous Propellant in a Rocket Motor," *Combustion and Flame*, Vol. 96, No. 2, 1994, pp. 325–342.